ApJ (Main Journal); accepted September 3, 1997

A very low mass of ^{56}Ni in the ejecta of SN 1994W

Jesper Sollerman[1], Robert J. Cumming[1] and Peter Lundqvist[1,2]

ABSTRACT

We present spectroscopic and photometric observations of the luminous narrow-line Type IIP (plateau) supernova 1994W. After the plateau phase ($t \gtrsim 120$ days), the light curve dropped by ~ 3.5 mag in V in only 12 days. Between 125 and 197 days after explosion the supernova faded substantially faster than the decay rate of ^{56}Co, and by day 197 it was 3.6 magnitudes less luminous in R compared to SN 1987A. The low R-luminosity could indicate $\lesssim 0.0026^{+0.0017}_{-0.0011}$ $M_\odot$ of ^{56}Ni ejected at the explosion, but the emission between 125 and 197 days must then have been dominated by an additional power source, presumably circumstellar interaction. Alternatively, the late light curve was dominated by ^{56}Co decay. In this case, the mass of the ejected ^{56}Ni was $0.015^{+0.012}_{-0.008}$ $M_\odot$, and the rapid fading between 125 and 197 days was most likely due to dust formation. Though this value of the mass is higher than in the case with the additional power source, it is still lower than estimated for any previous Type II supernova.

Only progenitors with $M_{\rm ZAMS} \sim 8-10$ $M_\odot$ and $M_{\rm ZAMS} \gtrsim 25$ $M_\odot$ are expected to eject such low masses of ^{56}Ni. If $M_{\rm ZAMS} \sim 8-10$ $M_\odot$, the plateau phase indicates a low explosion energy, while for a progenitor with $M_{\rm ZAMS} \gtrsim 25$ $M_\odot$ the energy can be the canonical $\sim 10^{51}$ ergs. As SN 1994W was unusually luminous, the low-mass explosion may require an uncomfortably high efficiency in converting explosion energy into radiation. This favors a $M_{\rm ZAMS} \gtrsim 25$ $M_\odot$ progenitor.

The supernova's narrow (~ 1000 km s^{-1}) emission lines were excited by the hot supernova spectrum, rather than a circumstellar shock. The thin shell from which the lines originated was most likely accelerated by the radiation from the supernova.

Subject headings: supernovae: individual (SN 1994W) – abundances – gamma rays: theory – circumstellar matter – stars: neutron – black hole physics

[1]Stockholm Observatory, SE-133 36 Saltsjöbaden, Sweden.

[2]Send offprint requests to Peter Lundqvist; E-mail: peter@astro.su.se

1. Introduction

Type II supernovae (SNe II) are thought to arise from the explosion of massive ($M_{\rm ZAMS} \gtrsim 8 - 10\ M_\odot$) stars which end their lives with a substantial fraction of hydrogen in their envelopes. The explosion is triggered by the collapse of the progenitor's core. The best-understood core-collapse events are the SNe IIP (plateau), whose light curves are nearly flat during the first $\sim 2 - 4$ months. The long duration of the light curve plateau is believed to be due to the presence of a massive ($\gtrsim 2 - 3\ M_\odot$) hydrogen envelope (e.g., Falk & Arnett 1977).

After the plateau, the light curves of SNe IIP are often dominated by radioactive decay of ^{56}Co. The cobalt is the decay product of ^{56}Ni, and the luminosity at this epoch can therefore be used to estimate the amount of ^{56}Ni ejected at the explosion. Because the nickel is produced in the core region, the mass of ejected ^{56}Ni is an important probe of the core-collapse scenario itself, the nucleosynthetic yields of SNe II and their progenitors, and the nature of the compact central object formed at the collapse (Woosley & Weaver 1995; Woosley & Timmes 1996).

A new subclass of core-collapse supernovae has recently emerged: the narrow-line supernovae or SNe IIn (Schlegel 1990; Filippenko 1997). Like other SNe II they show strong Balmer lines, but the lines are narrow ($\sim 1000 - 3000$ km s^{-1}) and are seen in emission rather than absorption even at early times.

SN 1994W was discovered on 1994 July 29 in the Sbc galaxy NGC 4041 (Cortini & Villi 1994). Based on the presence of hydrogen lines it was quickly classified as a SN II (Bragaglia, Munari, & Barbon 1994). Subsequent spectroscopy showed that the lines had unusually narrow P-Cygni profiles ($v_{\rm FWHM} \sim 1200$ km s^{-1}) with broad emission wings, but no broad absorption component (Filippenko & Barth 1994; Cumming, Lundqvist, & Meikle 1994). Reports in IAU circulars indicated that the supernova reached a maximum of $V \sim 13.3$ around 1994 Aug 13. Further photometry by Tsvetkov (1995) showed that the supernova was a SN IIP, and had a remarkably sharp drop in the B and V light curves in early November 1994.

In this paper we present further photometric and spectroscopic observations of SN 1994W taken on several occasions between 1994 July 31 to 1996 April 20. We focus on the low luminosity of the supernova after ~ 120 days, and interpret this as due to an exceptionally low mass of ejected ^{56}Ni. We also discuss the formation of the narrow lines.

2. Observations

2.1. Photometry

Our photometric data were obtained mainly in R on six occasions from 1994 November 16 to 1996 April 20, using the Jakobus Kapteyn Telescope (JKT) and the Nordic Optical Telescope (NOT) on La Palma (see Table 1). The data were bias subtracted and flat fielded using standard

procedures within IRAF. Differential magnitudes between the supernova and comparison stars were measured using POLYFIT (Spännare 1997), which is a software package developed to do photometry on uneven backgrounds: a point spread function (PSF) is produced by fitting a Moffat function to an isolated star in the frame. This PSF and a polynomial fit to the background are then simultaneously fitted at the position of the object. For the JKT nights a bright comparison star was in the field and was used for the relative magnitudes. For the NOT data a fainter comparison star had to be used. Up to seven comparison stars were monitored to avoid variability. The comparison stars were calibrated against Landolt stars (Landolt 1983, 1992) at two nights on JKT and against a standard field in NGC 4147 (Christian et al. 1985) for the NOT observations. The zero point for the R magnitude differs slightly between the 4 photometric nights. We estimate a total systematic error of 0.15 mag in the R magnitude, including the neglect of color transformations and differential atmospheric extinction corrections, which were only applied to the day 646[3] data. For the V magnitude we calibrated relative to local standards measured by Tsvetkov (1995).

The JKT observations have rather low signal to noise or poor seeing, which gives large errors for the photometry, $\sim \pm 0.5$ mag. For the NOT observation (day 197) the error is smaller, and dominated by the error in the POLYFIT measurement. We estimated this error by adding to the image ten artificial stars of the same magnitude as the supernova at similar backgrounds using the IRAF task ADDSTAR. The rms error in the POLYFIT measurements of these were $\lesssim 0.15$ mag, which we regard as the measurement error also for the supernova. A total error of 0.3 mag on day 197 is therefore rather generous and includes errors for the comparison stars. At the last observation, day 646, the supernova was not detected. We estimated an upper limit by subtracting artificial PSFs of different brightness until a hole appeared in the background at the supernova position.

2.2. Spectroscopy

Our spectroscopic observations cover five epochs from day 18 to day 202 (see Table 2). The data were bias subtracted, flat fielded and wavelength calibrated using IRAF. The day 31, 57 and 202 spectra were flux calibrated against a spectrophotometric standard star. The day 57 spectrum was taken at high airmass and required further corrections for slit losses. A rough flux calibration for the day 18 spectrum was obtained by comparison with contemporary visual photometry and the spectrum on day 31. The day 121 spectrum was flux calibrated using the R photometry from day 125.

[3]Days are measured after 14.0 July, 1994 (see §3)

3. Results

In Figure 1 we present the light curve of SN 1994W. From the early R data, we estimate the date of optical outburst to have been 1994 July 14^{+2}_{-4}, and we label observations by number of days after this. The light curve shows a relatively gentle rise to maximum around 30 days, followed by a slow, plateau-like decline until ~ 110 days. The slow decline in B and V is typical of a SN IIP. At ~ 110 days, however, the supernova started to fade unprecedentedly fast, dropping by ~ 3.5 magnitudes in V in only 12 days. Also on the light curve tail, the fading continued at a fast rate, until our last photometric detection on day 197. We could not detect the supernova in V or R on day 646.

The spectrum of the supernova was also unusual for a SN II. Before the light curve drop, the spectra on days 18, 31 and 57 (see Figs. 2 and 3), show the strong P-Cygni lines of H I, typical of a SN II, but with very narrow profiles (minima at -700 km s^{-1} and maximum blue velocities of only 1000 km s^{-1}). In addition to the narrow features, the H I lines had emission wings extending out to ~ 5000 km s^{-1}, a factor of $\sim 2-4$ lower than the maximum velocities normally seen in SNe II at these epochs. The H I lines were accompanied by a rich spectrum of narrow lines of low-ionization species (He I, O I, Mg II, Si II, Fe II). Though conspicuous, the emission lines account for only $\sim 1\%$ of the total optical flux on days 31 and 57. Instead, a blue continuum dominates. Estimating $E(B-V) = 0.17 \pm 0.06$ from the interstellar Na I D absorption in our day 31 spectrum (Munari & Zwitter 1997), we fit it with blackbody spectra with temperatures of $\sim (1.50 \pm 0.15) \times 10^4$ K and $\sim (1.10 \pm 0.10) \times 10^4$ K, respectively. The effective temperatures indicated by the blackbody fits are much higher than the $\sim (5-8) \times 10^3$ K usually observed in SNe IIP at similar epochs.

The decrease in temperature was accompanied by the disappearance of the He I lines and increasingly strong Fe II features. A spectrum taken by Filippenko (1997) on day 80 shows that the spectral features had changed only marginally compared to our day 57 spectrum, but the slope of the continuum indicated a decrease in effective temperature to $\sim (7-8) \times 10^3$ K.

The photometric fading at $\sim$110 days coincided with dramatic changes in the spectrum. The $B-V$ color, previously steady at 0.3 ± 0.1, increased to 1.75 between days 85 and 111 (Fig. 1; Tsvetkov 1995). In addition, the flux in Hα dropped at roughly the same rate as the V and R light curves. This coincidence, together with the shift to lower-excitation lines during the plateau phase, suggests that the narrow lines were predominantly excited by the supernova continuum rather than by a circumstellar shock (see §4.4).

The day 121 spectrum shows narrow ($\sim 730 \pm 120$ km s^{-1}) emission in Hα, Na I D λ5893 and [Ca II] $\lambda\lambda$7291, 7324, on top of a continuum-like spectrum. The flux of the narrow Hα component had dropped by a factor ~ 150 since day 57. No broad features can be identified, but the sharp edge present at ~ 5600 Å is a common feature in late-time supernova spectra, usually attributed to the redmost extent of blended Fe II or [Fe II] lines. We suggest that the apparent continuum is in fact made up of overlapping broad emission lines, with a gap around 5650 Å. Unlike other Type

II events at this epoch, there is no sign of strong, broad Hα.

On day 202, the spectrum was dominated by a fairly flat, noisy continuum and unresolved Hα, which may contain a contribution from a background H II region. The flux in the narrow Hα line had dropped by a factor of $\gtrsim 5$ compared to the day 121 spectrum, but its width remained constant within the errors. The flux in the R band of our spectrum on day 202 agrees well with our R magnitude on day 197. Our photometric limit from day 646 ($R > 22$) demonstrates that the supernova continued to fade after day 202, and gives a lower limit on the flux contribution of the supernova to the day 202 spectrum of $\sim 50\%$. We suggest that the continuum at this epoch comes from background stars. We tentatively identify a broad, $v_{\rm FWHM} = (4.5 \pm 1.5) \times 10^3$ km s^{-1}, emission feature at ~ 7350 Å as [Ca II] $\lambda\lambda$7291, 7324, and suggest that the remaining emission left after the continuum is subtracted is, as on day 121, composed of broad emission lines. The [Ca II] feature has luminosity a factor of $\sim$100 lower than for SN 1987A at the same epoch; the luminosity of Hα is at least a factor of 2 lower still (Fig. 4).

4. Discussion

In Figure 5 we compare the absolute light curve of SN 1994W to those of other SNe IIP, SN 1987A and the luminous SN IIL (linear) 1979C. At maximum, SN 1994W was as luminous as SN 1983K, the most luminous SN IIP previously observed (Phillips et al. 1990). Evident from Figure 5 is the rapid fading and low luminosity of SN 1994W after the plateau phase ends, i.e., ~ 110 days, and the fast decline after that. We now investigate whether the unusual light curve and spectra of SN 1994W can be explained in terms of standard supernova theory.

4.1. The mass of ejected ^{56}Ni

For a SN IIP, the mass of ejected ^{56}Ni, $M_{\rm ej,56}$, can be estimated from the luminosity after the plateau phase ends. At this point the optical emission is powered by $\gamma-$ray energy deposited into the ejecta from the radioactive decay of ^{56}Co, the decay product of ^{56}Ni. The e-folding time for the cobalt decay is 111.26 days, so the radioactive decay creates a tail to the bolometric light curve with a slope of 0.00976 mag day^{-1}, if all the $\gamma-$rays are trapped. The luminosity of the tail gives a measure of $M_{\rm ej,56}$, when other contributions to the light curve have been accounted for.

The mass of ejected nickel has been determined in this way for a handful of SNe IIP, for example SNe 1969L (0.07 ± 0.03 $M_\odot$, Schmidt et al. 1993), 1990E ($0.073^{+0.018}_{-0.051}$ $M_\odot$, Schmidt et al. 1993), 1992H (~ 0.075 $M_\odot$, Clocchiatti et al. 1996) and SN 1991G ($0.024^{+0.018}_{-0.010}$ $M_\odot$, Blanton et al. 1995).

Our method to estimate $M_{\rm ej,56}$ of SN 1994W is to compare the level of its luminosity in R after the plateau to that of SN 1987A at similar epochs. We choose SN 1987A as a template since

its distance and extinction are well known, and because its light curve was entirely powered by radioactive decay as soon as a few days after explosion. SN 1987A also resembled a SN IIP in that it had a massive hydrogen envelope (Woosley 1988). For SN 1987A the value of $M_{\rm ej,56}$ was $\sim 0.071^{+0.019}_{-0.016}\ M_\odot$ (Suntzeff & Bouchet 1990).

A problem with our method is that the light curve tail of SN 1994W declines substantially faster than the decay rate of ^{56}Co. We must therefore be careful in spelling out the assumptions involved in interpreting the light curve. We identify two possible scenarios which can lead to such a decline, and which lead to different estimates of $M_{\rm ej,56}$. Radioactive decay of ^{56}Co could dominate, but be unable for some reason to maintain the standard tail of the R light curve. Alternatively, some source other than ^{56}Co decay dominates the light curve during this period. In the following sections we investigate both these possibilities and their implications for $M_{\rm ej,56}$.

4.2. The steep decline of the late light curve: implications for the nickel mass

First we consider the possibility that all of the flux on the tail was indeed due to cobalt decay. The steep decline could then be due to increasing escape of γ-rays, a gradual shift of the spectrum from the optical to the infrared, or increasing dust obscuration.

Assuming a central radioactive source, the optical depth to γ-rays through the ejecta decreases with time as $\tau_\gamma = (t_1/t)^2$, where t_1 is the time when $\tau_\gamma = 1$. In SN 1987A, $t_1 \sim 750$ days (Kozma 1996). Including the fact that $\sim 3.5\%$ of the cobalt decay energy is mediated by positrons and therefore deposited locally, the bolometric luminosity decays by the factor $f_{\rm leak} = (1 - 0.965\ \exp(-\tau_\gamma))$ in addition to the decay of ^{56}Co. The observed flux in R between days 125 and 197 drops by a factor $f_{\rm obs} = 6.6^{+7.2}_{-3.5}$ in addition to cobalt decay. With the assumptions above the maximum value of $f_{\rm leak}$ for the same period is only 2.0 (for $t_1 \sim 77$ days) and thus cannot reproduce the fast decline of the light curve. We therefore believe that γ-ray leakage was not the cause of the exceptionally fast fading of SN 1994W after ~ 120 days.

A gradual shift of the spectrum into the infrared might be expected if the mass of ^{56}Ni was substantially lower than in SN 1987A, and the reduced radioactive heating lowered the ejecta temperature. In this scenario our assumption of linear scaling between $M_{\rm ej,56}$ and the R-luminosity could break down. To test this numerically, we ran two models of SN 1987A kindly provided for us by C. Kozma. These models do not include dust formation and are similar to her mixed 10H model in Kozma (1996), but with only $M_{\rm ej,56} = 0.001$ (0.01) $M_\odot$, and with other radioactive isotopes decreased accordingly. We find that on day 150, more than 60 (70)% of the line emission comes out between $3000 - 9000$ Å, $\sim 7.3(5.3)\%$ and $\sim 6.6(2.2)\%$ of which in Hα and [Ca II], respectively. Therefore, if dust formation is unimportant, and the structure similar to that of SN 1987A, linear scaling of $M_{\rm ej,56}$ with R and V luminosities seems to be valid down to very low values of $M_{\rm ej,56}$.

The situation is different if dust formation is important. We expect that below some value of $M_{\rm ej,56}$, radioactive heating of the ejecta will be unable to prevent the formation of dust. This

could attenuate and shift the supernova emission into the infrared already shortly after the plateau phase. The effect could be further amplified by increased molecular cooling, since the destruction rate of molecules will decrease with lower $M_{\rm ej,56}$. We know that dust increased the cooling and obscured the line-emitting region in SN 1987A (Kozma 1996, and references therein), albeit at a later epoch (between $\sim 350 - 600$ days) than considered here for SN 1994W. The dust covering factor would have increased with time, creating a blueshift of the supernova lines, as observed for SN 1987A (Danziger et al. 1991). Our day 202 spectrum is too noisy to reveal such an effect. Thus, we cannot rule out dust formation as the cause of the fast fading in R.

To obtain an estimate of $M_{\rm ej,56}$ in the case of early dust formation, we choose the R measurement from day 139, which is the first photometric point on the light curve tail. This gives $M_{\rm ej,56} = 0.015^{+0.012}_{-0.008}\ M_\odot$. The estimated error includes the statistical error shown in Figure 1, uncertainty in the distance modulus of SN 1994W ($\pm$0.3 mag), the extinction towards the supernova ($\pm$0.15 mag) and an estimated systematic error of our R calibration ($\pm$0.15 mag).

This $M_{\rm ej,56}$ is slightly lower than for the previous record-holder, SN 1991G, which had $0.024^{+0.018}_{-0.010}\ M_\odot$. However, SN 1991G did not show the very steep decline of the light curve tail (Blanton et al. 1995). This could mean that even SN 1991G ejected too much ^{56}Ni to allow early dust formation, though the structure of SN 1991G could also have been less favorable for dust formation to occur than in SN 1994W.

If the steep tail is not primarily powered by radioactive decay we need an additional, fast declining, energy source. A light echo seems rather improbable as it would produce a spectrum on the tail that is qualitatively similar to the spectrum at the peak. This is not observed. A more attractive power source is interaction of the ejecta with circumstellar material at $\gtrsim 110$ days. In §4.4 we present evidence from the narrow line profiles for a thin, dense circumstellar shell close to the supernova. The high density we find for the shell may be sufficient to set up the isothermal-shock-wave scenario discussed by Grasberg & Nadyozhin (1986), in which the ejecta's kinetic energy is transformed to UV and optical emission. As the shell is accelerated, the conversion of kinetic energy becomes less efficient, which could create the steeply-falling light curve. In this case the photometric point on day 197 gives a firm upper limit to $M_{\rm ej,56}$. Assuming no dust, the γ-rays to be trapped and a linear scaling between R-luminosity and $M_{\rm ej,56}$ this gives $M_{\rm ej,56} \lesssim 0.0026^{+0.0017}_{-0.0011}\ M_\odot$. This limit could of course be higher if dust is important also in this scenario.

In summary, we suggest that the low luminosity on the light curve tail is due to a very low mass of ejected nickel.

4.3. The progenitor and the nature of the collapsed core

We will now examine whether such a small mass of ^{56}Ni can be consistent with the type of progenitor indicated by the light curve up to ~ 110 days. The very low nickel mass we find, if

radioactivity is not the prime power source between days 120 and 197 ($M_{\rm ej,56} \lesssim 0.0026^{+0.0017}_{-0.0011}\ M_\odot$), agrees with model calculations only for progenitors in the ranges $M_{\rm ZAMS} \sim 8 - 10\ M_\odot$ (Mayle & Wilson 1988) and $M_{\rm ZAMS} \gtrsim 25\ M_\odot$ (Woosley & Weaver 1995). If the steep decline of the light curve tail was due instead to early dust formation, our more conservative estimate ($M_{\rm ej,56} = 0.015^{+0.012}_{-0.008}\ M_\odot$) is still lower than the range $M_{\rm ej,56} \sim 0.04 - 0.20\ M_\odot$, predicted for progenitors in the range $M_{\rm ZAMS} \sim 11 - 25\ M_\odot$ (Woosley & Weaver 1995), but somewhat higher than $M_{\rm ej,56}$ predicted for stars with $M_{\rm ZAMS} \sim 8 - 10\ M_\odot$ (Mayle & Wilson 1988).

Theory thus favors two kinds of progenitor that eject low masses of ^{56}Ni: a low mass progenitor, that produces almost no nickel during the explosion, or a very massive star where the mass-cut (the location in mass coordinates between ejected matter and that eventually forming the compact, central object) is situated sufficiently far out for most of the synthesized nickel to be trapped in the compact object. Due to the extensive fall-back of material in the latter case, the mass of the compact object may become large enough to form a black hole (Woosley & Timmes 1996). As a matter of fact, Woosley & Timmes (1996) suggested that the prime observational diagnostic of a supernova forming a black hole would be a bright supernova that plummeted to very low or zero luminosity right after the plateau.

To estimate the mass of the progenitor we use the early light curve (i.e., at $t \lesssim 110$ days) of the supernova. At this epoch the supernova is powered by the release of stored shock energy from the explosion. The physics of the plateau phase has been parameterized analytically (Popov 1993) and fitted to numerical simulations (Litvinova & Nadyozhin 1985) in terms of the explosion energy, E, the stellar radius, R_0, and the mass of the hydrogen envelope at the time of explosion, $M_{\rm env}$. Assuming a canonical value for E in the range $(1.0 - 1.5) \times 10^{51}$ ergs, we use parameterized expressions to estimate R_0 and $M_{\rm env}$ for given $t_{\rm d}$ (the epoch when the plateau ends) and V (the absolute visual magnitude before turn-down). Taking $t_{\rm d} \sim 110$ days and $V = -17.7 \pm 0.5$, Popov's expressions give $M_{\rm env} \sim 7 - 13\ M_\odot$ and $R_0 \sim (0.5 - 2.0) \times 10^{14}$ cm, while the numerical models of Litvinova & Nadyozhin give $M_{\rm env} \sim 11 - 19\ M_\odot$ and $R_0 \sim (0.4 - 1.2) \times 10^{14}$ cm. $M_{\rm env}$ decreases with increasing R_0 for given V and E. We thus derive a value of $M_{\rm env}$ which is similar to, or in the case of the numerical models, slightly higher than that of SN 1987A (Woosley 1988; Shigeyama & Nomoto 1990).

Such high values of $M_{\rm env}$ strongly favor the higher mass range ($M_{\rm ZAMS} \gtrsim 25\ M_\odot$) for the progenitor of SN 1994W. To $M_{\rm env}$ we need to add the mass of the helium- and metal-rich core at the time of explosion. For a progenitor with $M_{\rm ZAMS} = 25\ M_\odot$, this is $\sim 9\ M_\odot$ (Woosley & Weaver 1995). To be consistent with our estimate of $M_{\rm env}$ for a $M_{\rm ZAMS} = 25\ M_\odot$ progenitor, we must therefore allow for $3 - 9\ M_\odot$ of stellar winds if Popov's expressions are used for the plateau, while the numerical models do not require presupernova mass loss.

A low-mass ($M_{\rm ZAMS} \sim 8 - 10\ M_\odot$) progenitor is possible for SN 1994W, but only if the explosion energy was lower than the canonical $(1.0 - 1.5) \times 10^{51}$ ergs assumed above and the conversion of explosion energy to radiation was very efficient. Model B of Falk & Arnett (1977)

shows that a high ($> 30\%$) efficiency is possible if the star is very extended ($R_0 = 9.25 \times 10^{14}$ cm). Assuming an explosion energy as low as 3×10^{50} ergs, Popov's model can give an envelope mass of only $\sim 3.5\ M_\odot$ for a radius of 5×10^{14} cm, while the model of Litvinova & Nadyozhin gives $\sim 5.0\ M_\odot$ for a radius of 3×10^{14} cm. Both the analytical and numerical estimates are thus consistent with a low mass ($M_{\rm ZAMS} \sim 8 - 10\ M_\odot$) progenitor, if the progenitor is very extended and the explosion energy is low. Because a $M_{\rm ZAMS} \sim 8 - 10\ M_\odot$ supernova only ejects $M_{\rm ej,56} \sim 0.002\ M_\odot$ (Mayle & Wilson 1988), this type of explosion is consistent only with our lowest $M_{\rm ej,56}$ (see §4.2).

If SN 1994W resulted from the explosion of an $8 - 10\ M_\odot$ star, its compact object should be a neutron star. If its progenitor was instead in the higher range, the mass of the newly-created compact object could become large enough to form a black hole (Woosley & Timmes 1996). For a $25\ M_\odot$ progenitor, the mass-cut should be $\gtrsim 2.1\ M_\odot$ (Timmes, Woosley & Weaver 1996). The maximum mass of a neutron star is rather uncertain, depending on the adopted equation of state. If it is as low as $\sim 1.5 - 1.6\ M_\odot$ (Brown & Bethe 1994), such a massive progenitor for SN 1994W most likely formed a black hole.

4.4. The narrow lines

The narrow lines of SN 1994W are not typical for SNe IIP. In §3 we argued that the flux in the lines was too low to affect the light curve on the plateau, which is why we were able to apply the light curve analysis in §4.3. Here we discuss the origin of the narrow lines. As already suggested in §3, the lines are naturally explained in terms of excitation by the hot supernova continuum. Another possibility could be excitation caused by circumstellar interaction of the ejecta with a clumpy wind, as suggested for SN 1988Z by Chugai & Danziger (1994). However, we see no obvious reason why this excitation mechanism should result in an excitation of the lines that closely follows the fading of the supernova continuum as in SN 1994W.

The narrow emission lines were present as early as day $17 - 18$ (Bragaglia et al. 1994, Cumming et al. 1994). Hα had a roughly constant P-Cygni profile from then until at least day 57, the epoch of our last spectrum on the plateau (see Fig. 3). The emission part of the P-Cygni profile has a rounded rather than flat-topped peak, which immediately indicates that the optical depth in the lines $\gg 1$ (Mihalas 1978). Furthermore, the steep red side and relatively broad absorption trough observed in both H I and Fe II indicate that the lines were scattering-dominated, and originated in a rather thin shell ($\Delta R/R < 1$) located close to the photosphere (see Fransson 1984). The optical thickness of the Fe II lines allows us to put a limit on the density in the shell. Assuming a gas temperature of 10^4 K and Fe II/H = Fe/H = 4×10^{-5} (i.e., the solar value of Fe/H), we use expressions from Mihalas (1978) to obtain a hydrogen density $n_{\rm H} \gg 3 \times 10^8\ v_3\ r_{15}^{-1}$ cm^{-3}. Here, v_3 is the velocity of the shell in units of 10^3 km s^{-1} and r_{15} the shell radius in units of 10^{15} cm. We know from the line profiles that $v \sim 10^3$ km s^{-1}, and that the shell radius must be close to that of the photosphere. From our blackbody fits (see §3) we estimate that the photospheric radius

on days 31 and 57 was $\sim 8.5 \times 10^{14}$ cm and $\sim 1.1 \times 10^{15}$ cm, respectively. This gives a limit on $n_{\rm H} \gg 3 \times 10^8$ cm^{-3}, quite consistent with the absence of forbidden lines in the spectrum during the plateau.

The near-constancy of the shell's velocity up to day 57 and its proximity to the photosphere allow us to locate the starting radius of the shell, r_0, assuming it is the same shell that emits the lines at all epochs. Using $v_3 = 1$, we obtain $r_0 \sim 6 \times 10^{14}$ cm from both the day 31 and day 57 data. Because the radius of the photosphere is rather uncertain ($\sim \pm 30\%$), so is r_0.

The shell appears to have been quite close to the supernova around the time of explosion. We identify two possible origins. One possibility is that the shell was created in the supernova envelope during the explosion. The formation of such a shell was suggested by Falk & Arnett (1977), who actually also predicted that this should result in narrow P-Cygni profiles. The problem with this interpretation is the low velocity of the shell. Even in their low-explosion-energy, extended model B, Falk & Arnett find a shell velocity roughly twice as high as we find for SN 1994W.

It seems more plausible that the shell was circumstellar, perhaps due to an episode of increased mass loss some time $t = (r_0 - R_0)/v_{\rm sh}$ prior to the explosion, where $v_{\rm sh}$ is the initial velocity of the shell. This scenario is similar to the model presented by Grasberg & Nadyozhin (1986) for SN 1983K. We find that the radiation from the supernova can easily accelerate the shell to the observed velocity. Assuming pure electron scattering, a shell initially at rest is accelerated up to $v \sim 8.9 \times 10^2 \; L_{50} \; r_{15}^{-2}$ km s^{-1}, where L_{50} is the integrated bolometric luminosity of the supernova in units of 10^{50} ergs and r_{15} the shell radius in units of 10^{15} cm. The velocity can be substantially higher if line acceleration is important. We note that the blue edge of the Hα absorption shifted slightly to the blue between days 18 and 31, corresponding to an increase in shell velocity from 997 ± 30 km s^{-1} to 1063 ± 15 km s^{-1} (Fig. 3). This is consistent with the supernova radiation continuing to accelerate the shell between these epochs.

In the model of Grasberg & Nadyozhin (1986), the shell is eventually accelerated to the velocity of the supernova ejecta due to circumstellar interaction. However, in reality this may take longer than in Grasberg & Nadyozhin's 1-D models because the slow shell might break up (Falk & Arnett 1977). In SN 1994W, the disruption of the proposed shell by the ejecta could perhaps power the light curve between ~ 120 and 197 days, as we suggested in §4.2.

5. Conclusions

We have observed the luminous SN 1994W. We find that the low flux of the supernova after ~ 120 days is evidence of very low mass of ^{56}Ni ejected at the explosion, in fact the lowest inferred for any SN II.

The estimated mass of ^{56}Ni depends on the interpretation of the unusually rapid fading observed in R between days 120 and 197. Either the supernova ejected $0.015^{+0.012}_{-0.008}$ $M_\odot$ of ^{56}Ni,

or the nickel mass could have been as low as $\lesssim 0.0026^{+0.0017}_{-0.0011}\ M_\odot$. The first possibility requires inefficiency in converting radioactive decay energy to R luminosity, and we find that early dust formation is the most likely cause for this. Alternatively, the primary power source between $120 - 197$ days was not radioactive decay, but perhaps interaction with a thin circumstellar shell. In this case $M_{\rm ej,56} \sim 0.0026^{+0.0017}_{-0.0011}\ M_\odot$ is an upper limit, if dust formation was unimportant.

Two types of progenitor seem consistent with the low nickel content and high luminosity of the supernova before the end of its plateau phase. The first possibility is a low mass progenitor with $M_{\rm ZAMS} \sim 8 - 10\ M_\odot$, which had a very extended envelope and a low explosion energy, $E \sim 3 \times 10^{50}$ ergs. As a low mass progenitor only produces $\sim 0.002\ M_\odot$ ^{56}Ni (Mayle & Wilson 1988), consistent only with our lowest value for $M_{\rm ej,56}$, an additional power source, presumably circumstellar interaction, is needed to explain the light curve between $120 - 197$ days for this type of progenitor. However, the energy budget seems uncomfortably tight for the low-mass case as SN 1994W was one of the most luminous supernovae observed.

A more natural possibility is therefore a high mass progenitor with $M_{\rm ZAMS} \gtrsim 25\ M_\odot$, which could have lost a few solar masses as stellar winds, and exploded with the canonical energy $(1.0 - 1.5) \times 10^{51}$ ergs. This type of progenitor is consistent with both our estimates of $M_{\rm ej,56}$. Such a supernova should have a mass-cut $\gtrsim 2.1\ M_\odot$, sufficient to trap most of the produced ^{56}Ni, and could have formed a black hole.

Finally, we find that the narrow lines were formed in a thin, circumstellar high-density shell close to the supernova, accelerated by the radiation from the supernova.

We thank P. Rudd, R. Rutten, M. Breare and E. Harlaftis for taking service observations, E. Zuiderwijk for giving up PATT time to take the day 18 spectrum, and M. Näslund for taking part in our last observation of the supernova. We are especially grateful to C. Kozma, B. Leibundgut and S. Blinnikov for important discussions, and to L. Szentasko and M. Villi for access to unpublished data. We also thank M. Pérez-Torres for early analysis of the narrow lines and S. Spännare for help with photometry measurements. This research was supported by the Swedish Natural Science Research Council. JS and PL also acknowledge support from the Swedish National Space Board.

REFERENCES

Blanton, E. L., Schmidt, B. P., Kirshner, R. P., Ford, C. H., Chromey, & F. R., Herbst, W. 1995, AJ, 110, 2868

Bragaglia, A., Munari, U., & Barbon, R. 1994, IAU Circ., No. 6044

Brown, G. E., & Bethe, H. A. 1994, ApJ, 423, 659

Chugai, N. N., & Danziger, I. J. 1994, MNRAS, 268, 173

Clocchiatti, A. et al. 1996, AJ, 111, 1287

Cortini, G., & Villi, M. 1994, IAU Circ., No. 6042

Christian, C. A., Adams, M., Barnes, J. V., Buthcher, H., Hayes, D. S., Mould, J. R., & Siegel, M. 1985, PASP, 97, 363

Cumming, R. J., Lundqvist, P., & Meikle, W. P. S. 1994, IAU Circ., No. 6057

Danziger, I. J., Bouchet, P., Gouiffes, C., & Lucy, L. B. 1991, in Proc. ESO/EIPC Supernova Workshop, SN 1987A and other Supernovae, eds. I. J. Danziger & K. Kjär, (Garching: ESO), 217

Falk, S. W., & Arnett, W. D. 1977, ApJS, 33, 515

Ferrarese, L. et al. 1996, ApJ, 464, 568

Filippenko, A. V. 1997, ARA&A, in press

Filippenko, A. V., & Barth, A. J. 1994, IAU Circ., No. 6046

Fransson, C. 1984, A&A, 132, 115

Grasberg D. K., É. K, & Nadyozhin 1986, Pis'ma AZh, 12, 168

Kozma, C. 1996, Ph.D. Thesis (Stockholm University)

Kraan-Korteweg, R. C. 1986, A&AS, 66, 255

Landolt, A. 1983, AJ, 88, 439

Landolt, A. 1992, AJ, 104, 340

Litvinova, I. Yu., & Nadyozhin, D. K. 1985, Pis'ma AZh, 11, 351

Mayle, R., & Wilson, J. R. 1988, ApJ, 334, 909

Mihalas, D. 1978, Stellar Atmospheres (2nd ed.; San Francisco: Freeman)

Munari, U., & Zwitter, T. 1997, A&A, 318, 269

Phillips, M. M., Hamuy, M., Maza, J., Ruiz, M. T., Carney, B. N., & Graham, J. A. 1990, PASP, 102, 299

Popov, D. W. 1993, ApJ, 414, 712

Richmond, M. W., Treffers, R. R., Filippenko, A. V., & Van Dyk, S. D. 1994, IAU Circ., No. 6043

Schlegel, E. M. 1990, MNRAS, 244, 269

Schmidt, B. P. et al. 1993, AJ, 105, 2236

Shigeyama, T., & Nomoto, K. 1990, ApJ, 360, 242

Spännare, S. 1997, Ph.Licentiate Thesis (University of Lund)

Suntzeff, N. B., & Bouchet, P. 1990, AJ, 99, 650

Timmes, F. X., Woosley, S. W., & Weaver, T. A. 1996, ApJ, 457, 834

Tsvetkov, D. Yu 1995, Information Bull. Variable Stars, 4523, 1

Tully, R. B. 1988, Nearby Galaxies Catalog, Cambridge University Press

Woosley, S. E. 1988, ApJ, 330, 218

Woosley, S. W., & Timmes, F. X. 1996, Nucl. Phys. A, 606, 137

Woosley, S. W., & Weaver, T. A. 1995, ApJS, 101, 181

Table 1. Supernova 1994W - log of photometric observations

date	day [1]	telescope/ instrument	bandpass	magnitude	observer(s)
941116.2	125	JKT/TEK4	V	19.0±0.2	P. Rudd
			R	18.4±0.5	P. Rudd
941130.3	139	JKT/TEK4	R	18.8±0.5	V. Dhillon
941222.3	161	JKT/TEK4	R	19.7±0.6	E. Harlaftis
950120.3	190	JKT/TEK4	R	20.7±0.6	E. Harlaftis
950127.3	197	NOT/STANCAM1	R	21.15±0.3	J. Sollerman, R. Cumming
960420.0	646	NOT/BROCAM2	R	> 22	J. Sollerman, M. Näslund

Note. — Observations at the Jakobus Kapteyn Telescope (JKT) were taken during service time.

[1]Days since July 14.0, 1994.

Table 2. Supernova 1994W - log of spectroscopic observations

date	day [1]	telescope/ instrument	wavelength region (Å)	resolution (Å)	observer(s)
940731.9	18	INT/IDS	6507-6675	0.25	E. Zuiderwijk
940813.9	31	WHT/ISIS	4290-8005	2.7	M. Breare
940908.9	57	WHT/ISIS	3300-9360	11	R. Rutten
940908.9	57	WHT/ISIS	4255-5060,6345-7150	2.7	R. Rutten
941112.3	121	INT/IDS	5485-7370	6	R. Rutten
950201.5	202	NOT/LDS	4800-10000	12	R. Cumming, J. Sollerman

Note. — Observations at William Herschel Telescope (WHT) and Isaac Newton Telescope (INT) were taken during service time. The Nordic Optical Telescope (NOT) observations were made by the authors.

[1]Days since July 14.0, 1994.

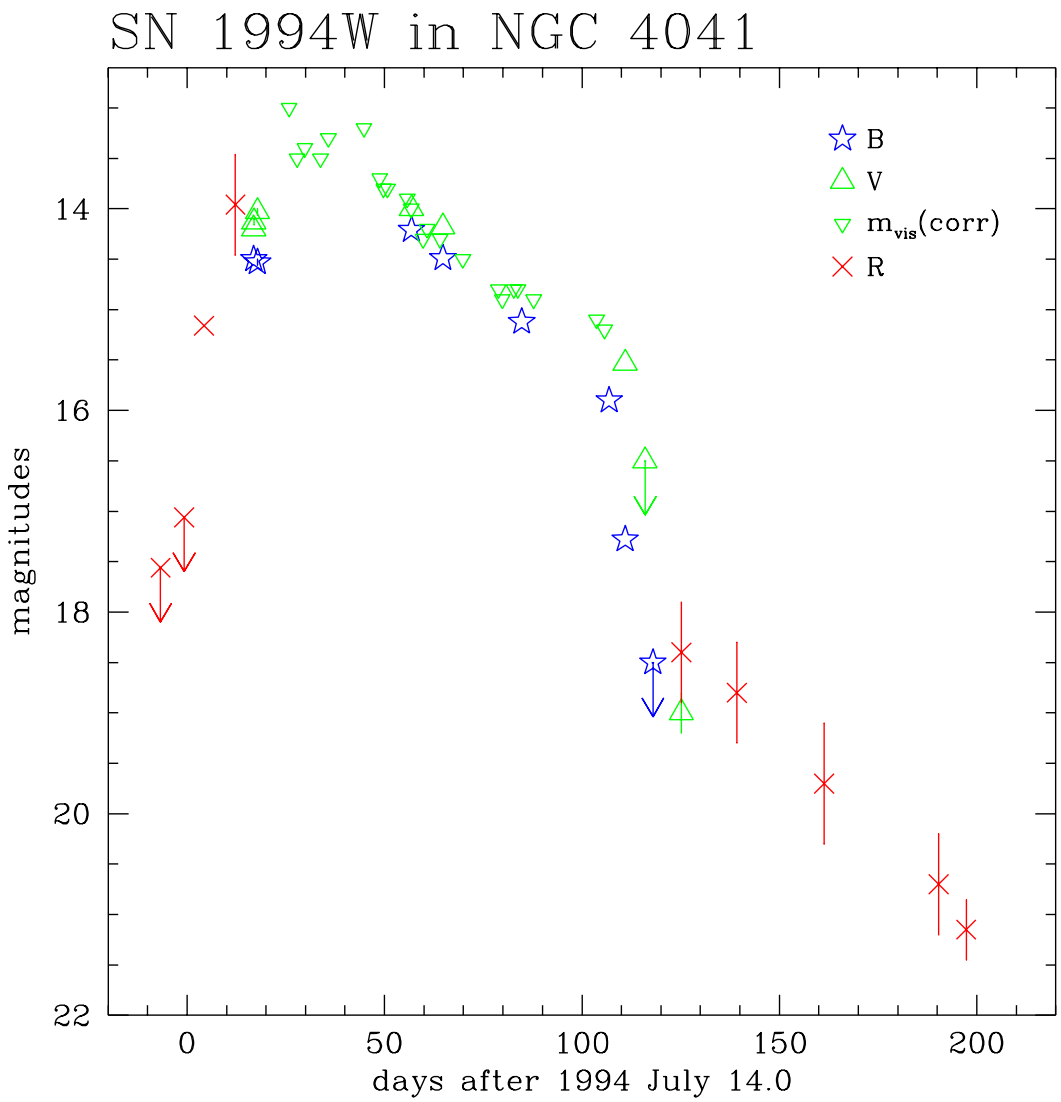

Fig. 1.— Observed B, V and R light curves of SN 1994W. The data set is a compilation of our own CCD photometry (Table 1), plus photoelectric and photographic photometry compiled from Tsvetkov (1995), IAU circulars, and the observations of L. Szentasko and M. Villi (priv. comm.; inverted triangles). We compared Szentasko's and Villi's estimates for this supernova, and for SNe 1994D and 1994I (from the unpublished lists compiled by B. H. Granslo) with contemporary V and $B-V$ measurements where they were available. Szentasko's values for all three SNe required a correction of -0.5±0.2 mag to match them with V. There was no noticeable color term. The corrected magnitudes follow the photoelectric V points well. The early R points were derived from the relative photometry of Richmond et al. (1994), using our measurement of $R = 13.96 \pm 0.15$ for their nearby calibration star (Tsvetkov's star 3).

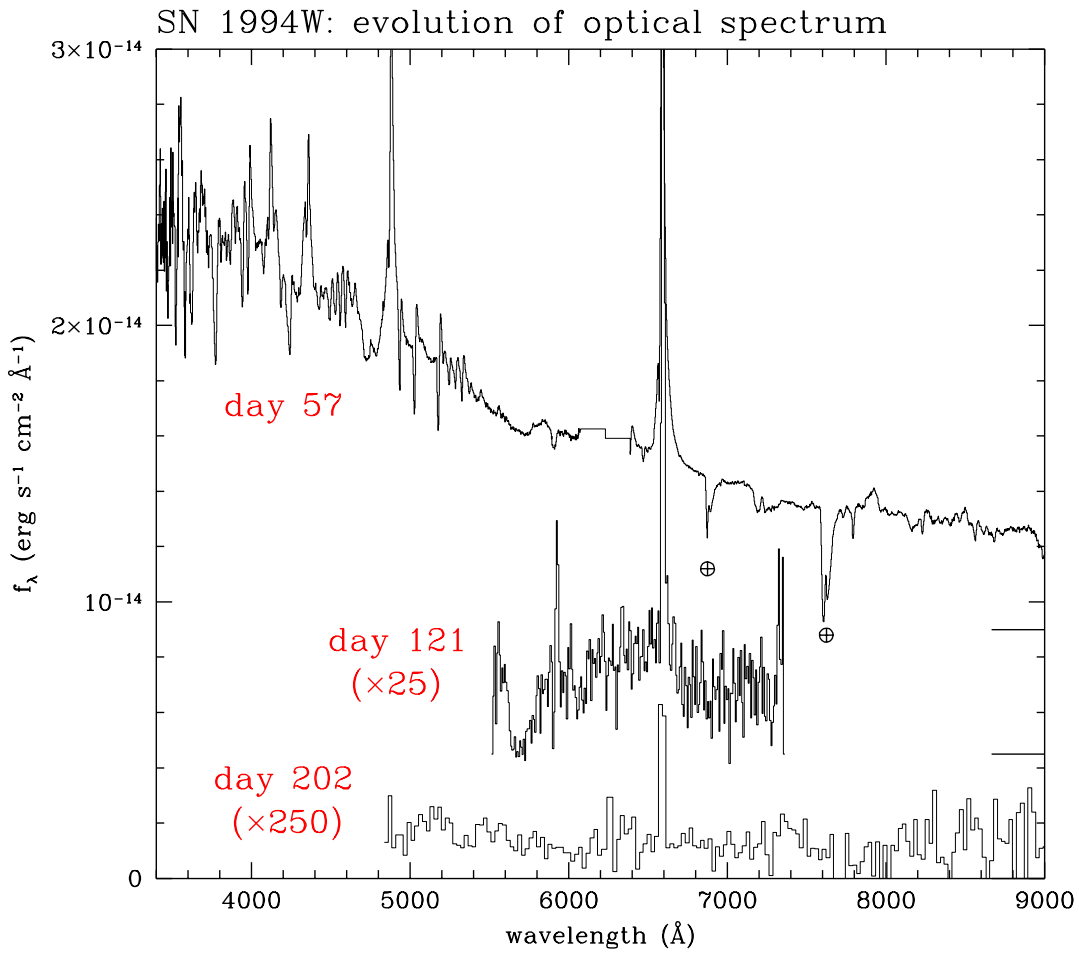

Fig. 2.— Spectra of SN 1994W at 57, 121 and 202 days after explosion. The two long tick marks to the right show the level of zero flux at 57 and 121 days.

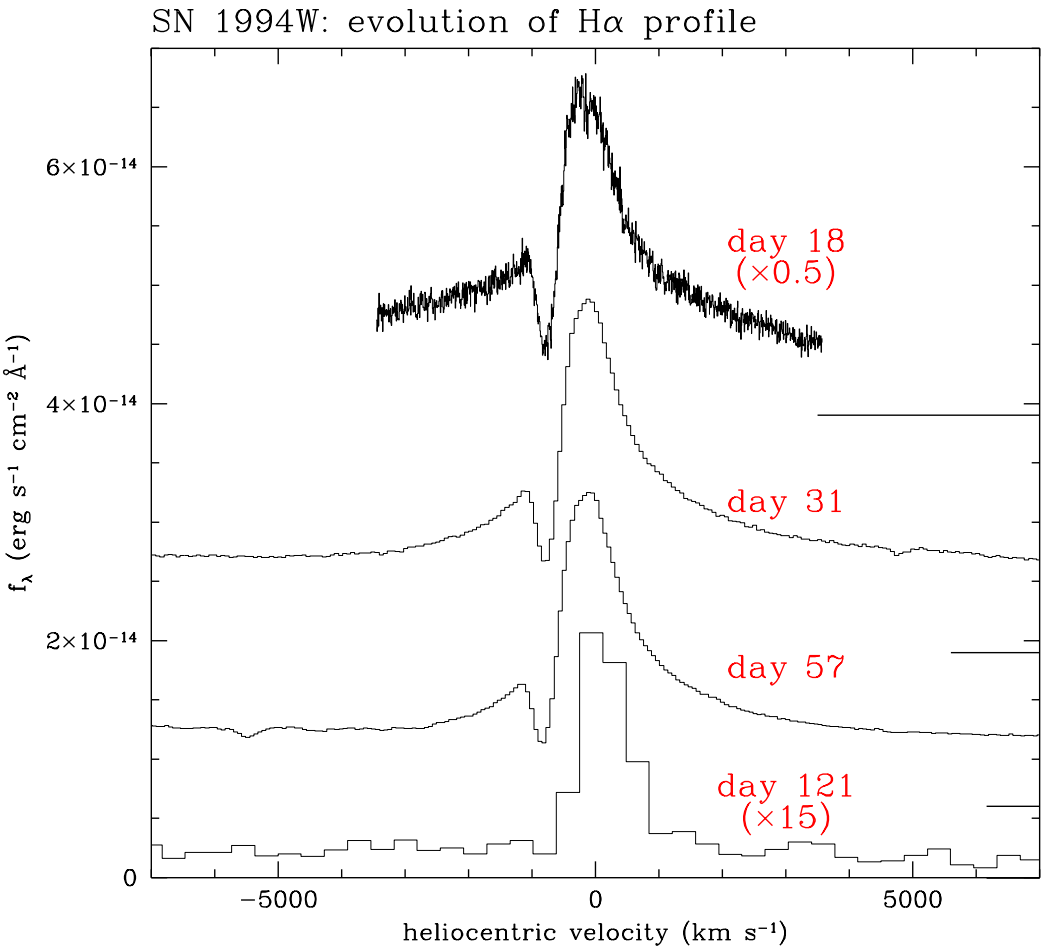

Fig. 3.— Evolution of the Hα line profile of SN 1994W from day 18 to day 121. Note the near constancy of the position of the blue edge of the absorption. The three long tick marks to the right show the level of zero flux at 18, 31 and 57 days.

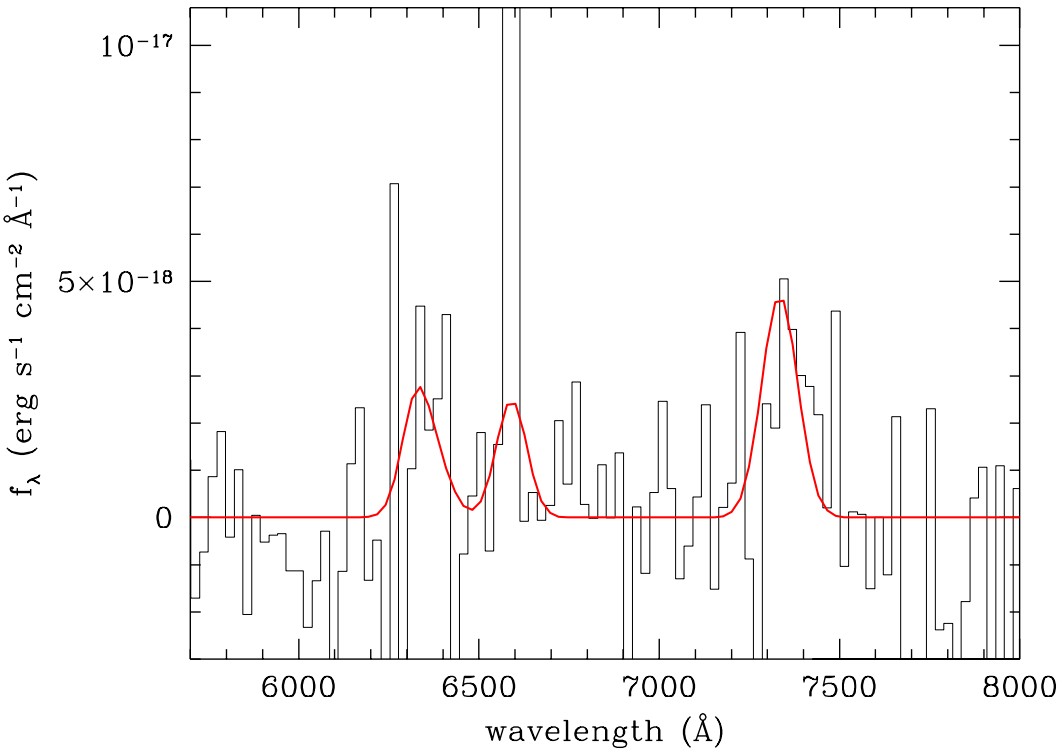

Fig. 4.— Spectrum of SN 1994W at day 202, with continuum subtracted. The solid line (not a fit to the spectrum) shows gaussian profiles of width 4500 km s^{-1} at the positions of [O I] $\lambda\lambda$6300, 6364, Hα and [Ca II] $\lambda\lambda$7291, 7323 in the ratio 3: 1: 2.5: 3: 2.

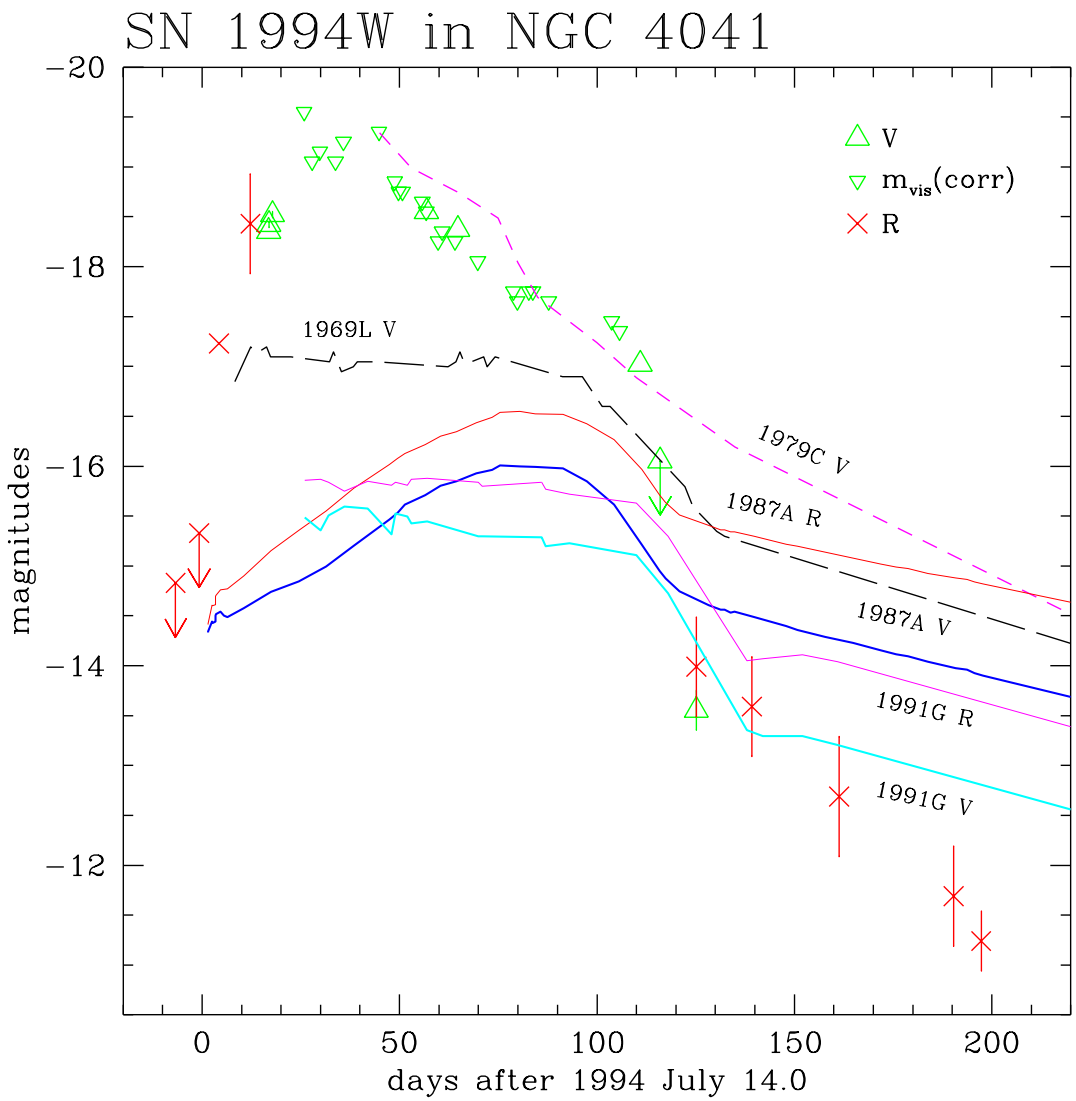

Fig. 5.— Absolute light curves of SN 1994W compared with selected other Type II supernovae. We adopt 25.4 Mpc for the distance to SN 1994W (taking recession velocity of 1231 km s^{-1} from Tully (1988) and adopting $H_0 = 65$ km s^{-1} Mpc^{-1} with the Virgo infall model of Kraan-Korteweg [1986]). Using the relations of Munari & Zwitter (1997) for the strength of interstellar Na I absorption, we estimated the extinction towards SN 1994W to be $E(B-V)$=0.17±0.06. For the other SNe the following original data were adopted: SN 1969L (distance 11 Mpc; A_V 0.19 mag; Schmidt et al. 1993); 1979C (16.1 Mpc; 0.45 mag; Ferrarese et al. 1997); 1987A (50 kpc; 0.15 mag; Suntzeff & Bouchet 1990); 1990E (21 Mpc; 1.5 mag; Schmidt et al. 1993); 1991G (15.5 Mpc; 0.025 mag; Blanton et al. 1995).